VIP Molecular Complexes

DOI: 10.1002/anie.200603809

Lock-and-Key Principle on a Microscopic Scale: The Case of the Propylene Oxide···Ethanol Complex**

*Nicole Borho and Yunjie Xu**

The introduction of the lock-and-key principle to explain the specificity of enzyme reactions by Fischer in 1894,[1] has provided us a metaphor of molecular recognition, a fundamental mechanism utilized in almost all biological processes. A detailed description of the underlying intermolecular interactions of enzyme–substrate templates is, however, not yet fully accessible with simplified molecular modeling approaches currently used in virtual screening and rational drug design.[2,3] On the other hand, it is possible and of great interest to probe such recognition mechanism on the molecular level in a microscopic model system, which is amenable to high-level ab initio calculations. Here, we aim at a quantitative analysis of a microscopic lock-and-key model using pulsed-jet Fourier-transform microwave (FTMW) spectroscopy and ab initio methods. FTMW spectroscopy is known to provide accurate structural information and has the capability to distinguish conformers with minor geometric differences. It can also determine relative energies as small as one-tenth of a kcal mol^{-1},[4] leading to an experimental energetic ordering of the observed conformers. In particular, we seek to analyze the chiral discriminating forces at play in chiral molecular complexes. This phenomenon, known as chiral recognition,[5] occurs through multiple short-range stereospecific intermolecular interactions. They are responsible for the small energy difference between a homochiral (*R*,*R*′ or *S*,*S*′) and a heterochiral (*R*,*S*′ or *S*,*R*′) complex, termed chirodiastaltic energy (ΔE_{chir}).[5,6]

The phenomenon of chiral recognition has been the focus of several low-resolution spectroscopic studies based on UV/IR double resonance,[7] resonance-enhanced multiphoton ionization,[8] and broad-band FTIR spectroscopy.[9] Despite its great potential, high-resolution FTMW spectroscopy has only been utilized so far in three studies on chiral recognition. Howard and co-workers identified one heterochiral 2-butanol dimer[10] and three dimers of ethanol.[11] In a recent investigation, six homochiral and heterochiral conformers of the propylene oxide (PO) dimer were detected and the conformational stability of these conformers was determined.[12]

The 1:1 PO···EtOH complex was chosen based on the following four considerations: 1) amenability to high-level ab initio calculations; 2) a large dipole moment for FTMW measurements; 3) the presence of a strong primary hydrogen bond, leading to a limited number of stable conformers; and 4) chemical stability of the two binding partners. PO is a rigid chiral molecule and can be pictured as the solid "lock" in our lock-and-key metaphor. It can only act as a proton acceptor in a classic O–H···O hydrogen bond. EtOH, on the other hand, can adopt three different conformations: *gauche*+ (*G*+), *gauche*− (*G*−), and *trans* (*T*) with the H-O-C-C torsional angle at +60, −60, and 180 degrees, respectively. Although it does not have a permanent stereogenic center, the *G*− and *G*+ conformers are enantiomers to each other, related through helical chirality. They can interconvert through a tunneling process, which has been analyzed in detail by Pearson et al.[13] In the PO···EtOH hydrogen-bonded molecular adduct, one would expect the tunneling process to be quenched and the *G*+ and *G*− configurations to be locked in their respective spatial configurations. This phenomenon is termed transient chirality and has been observed experimentally by Hearn et al. in the formation of ethanol dimers.[11] The three EtOH configurations, that is, *G*+, *G*−, and *T*, can bind to the PO oxygen acceptor either on the same side of the PO methyl group (*syn*) or on the opposite side (*anti*). Consideration of both *R* and *S* enantiomers of PO leads to $3\times2\times2=12$ different structures, which form six pairs of enantiomers. As each (*R*)-PO···EtOH complex has a mirror image, (*S*)-PO···EtOH, and as both give rise to the same rotational spectrum, we use only one enantiomer, namely (*R*)-PO, throughout this study. A symbolic sketch of the six diastereomers is given in Figure 1. Here, we specify the (*R*)-PO···(*G*+)-EtOH complexes as homochiral, in which the stereocenters are of the same handedness, and the (*R*)-PO···(*G*−)-EtOH complexes as heterochiral.

To aid the spectral search, geometry optimizations of the PO···EtOH conformers were carried out using the Gaussian03 program package.[14] Six hydrogen-bonded conformers were located using second-order Møller-Plesset perturbation theory (MP2)[15] with the 6-311++G(d,p) basis set.[16] Harmonic frequency calculations were performed to obtain the zero-point energies (ZPEs) and to confirm the minimum nature of the conformers. Basis-set superposition error (BSSE) corrections were determined for the calculated dissociation energies using the counterpoise corrections of Boys and Bernardi.[17] Table 1 summarizes the calculated

[*] Dr. N. Borho, Prof. Dr. Y. Xu
Department of Chemistry
University of Alberta
Edmonton, AB, T6G 2G2 (Canada)
Fax: (+1) 780-492-8231
E-mail: yunjie.xu@ualberta.ca
Homepage: http://www.chem.ualberta.ca/~xu/

[**] This research was funded by the University of Alberta, the Natural Sciences and Engineering Research Council of Canada, the Canada Foundation for Innovation (New Opportunity), and an Alberta Ingenuity New Faculty Grant. We thank Z. Su for helpful discussions and W. Jäger for the instrument time on the microwave spectrometer. N.B. thanks the German Academic Exchange Service (DAAD) and Alberta Ingenuity for postdoctoral fellowships.

Supporting information for this article is available on the WWW under http://www.angewandte.org or from the author.

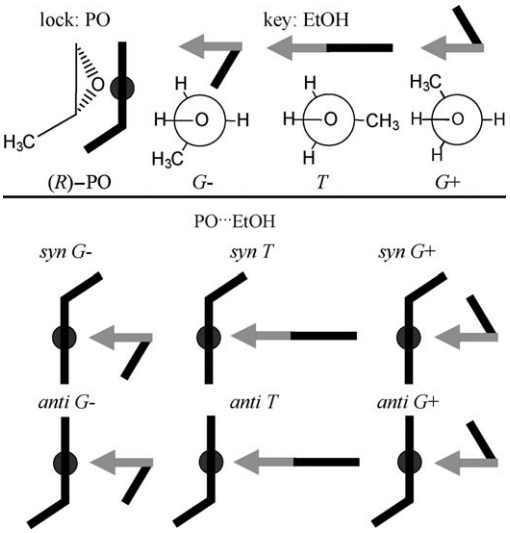

Figure 1. Schematic view of the propylene oxide (PO) monomer, the three conformations of EtOH, and the six conformers of the PO···EtOH complex as examples for the lock-and-key principle on a microscopic scale.

Table 1: Calculated dissociation energies (D_e) and ZPE-corrected dissociation energies (D_0), rotational constants (*A*, *B*, *C*), and electric dipole moment components ($|\mu_{a,b,c}|$) of the six most stable hydrogen-bonded conformers at the MP2/6-311++G(d,p) level of theory.[a]

Parameter	*syn G−*	*syn T*	*syn G+*	*anti G−*	*anti T*	*anti G+*
D_e	31.79	30.69	31.49	31.40	30.20	30.91
[kJ mol^{-1}]	(23.22)	(22.41)	(23.01)	(22.58)	(22.31)	(22.78)
D_0	25.03	24.77	24.75	24.80	24.53	24.43
[kJ mol^{-1}]	(16.47)	(16.50)	(16.27)	(15.98)	(16.63)	(16.30)
A [MHz]	4291	5217	4216	4025	7217	5846
B [MHz]	1182	926	1059	1205	782	963
C [MHz]	1009	848	1013	1000	761	892
$\|\mu_a\|$ [D]	1.99	2.25	2.48	2.53	1.96	1.92
$\|\mu_b\|$ [D]	1.68	0.65	0.58	1.47	0.34	1.53
$\|\mu_c\|$ [D]	0.64	0.69	0.55	0.41	0.33	0.45

[a] BSSE-corrected values are given in parentheses.

dissociation energies, rotational constants, and electric dipole moment components of the six conformers. The optimized geometries are displayed in Figure 2 together with the predicted relative energies. (The important intermolecular structural parameters of the six PO···EtOH conformers are listed in Table S1 in the Supporting Information). Despite the similarity of the OH···O primary interaction, the rotational constants of the conformers are predicted to be significantly different in most cases. This facilitates the identification and assignment of the different conformers when comparing the experimental rotational constants to the calculated ones. All conformers feature large *a* dipole moment components with magnitudes of 2–2.5 D, and three conformers, namely *anti G+*, *anti G−*, and *syn G−*, also exhibit appreciable *b* dipole moment components of about 1.5 D.

Thanks to substantial previous spectroscopic work, the manifold of lines originating from PO monomer,[18–20] EtOH monomer,[13,21] PO···^{20}Ne and PO···^{22}Ne complexes,[22,23] EtOH

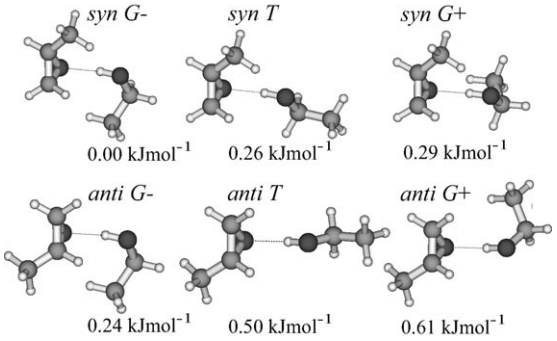

Figure 2. Structures and relative ZPE-corrected dissociation energies of the six most stable PO–EtOH conformers, calculated at the MP2/6-311++G(d,p) level of theory.

dimers,[11] and PO dimers,[12] which appear in the same spectral region as the PO···EtOH adduct, could be identified and excluded. As all the conformers are close to prolate symmetric tops, it was relatively straightforward to recognize the *a*-type transition patterns once the clutter of lines due to other species was removed. Fifteen to twenty-five *a*-type transitions were measured for each conformer. The frequencies of the *b*- and *c*-type transitions of each conformer were predicted from the preliminary semirigid rotor fits of the *a*-type transitions. Subsequently, a number of *b*- and *c*-type transitions were found and measured except in the case of the *anti T* conformer. The *anti T* conformer is predicted to have the smallest *b* and *c* dipole moment components and has an asymmetry parameter (κ value) of −0.993, closest to that of a prolate symmetric top (i.e. $\kappa = -1$), among the six conformers. There is therefore little information about the *A* rotational constant of *anti T* from the *a*-type transition fit. The observed transition frequencies of each conformer were fitted to a Watson's S-reduction semirigid rotor Hamiltonian in the I^r representation. The standard deviations of the fits are a few kHz, in good agreement with the experimental accuracy. Additionally, the rotational spectra of the singly deuterated PO···EtOD isotopomers were investigated. The resulting rotational and quartic centrifugal distortion constants of the parent and the deuterated isotopomers are summarized in Table 2. (The observed transition frequencies of both isotopomers of all six conformers are given in Table S3 in the Supporting Information). As the deuterium nuclear quadrupole hyperfine splittings were only partly resolved in most cases, no hyperfine structure analysis was performed and the frequencies of the strongest component were used in the rotational fits. The standard deviations are therefore slightly higher for the deuterated species.

It was noted that the *a*-type transitions of each D isotopomer were located about 1–20 MHz higher in frequency than that of the corresponding parent isotopomer, in contrast to the usual expectation of finding the heavier isotopomer at lower frequencies. The resulting *A* rotational constant of each D isotopomer decreases, while the *B* and *C* rotational constants increase. Such a reversed frequency pattern had been detected in the deuterated isotopomers of very weakly bound van der Waals complexes, such as Ne···H_2S and Ne···D_2S.[24] This was attributed to the effective zero-point vibrational

Table 2: Experimental spectroscopic constants[a] of the six conformers of the PO···EtOH adduct.[b]

Parameter	*syn G−*	*syn T*	*syn G+*	*anti G−*	*anti T*	*anti G+*
			H isotopomers			
A [MHz]	4300.6571(7)	5170.811(1)	4265.2770(7)	4019.8506(8)	7025(7)	5863.279(1)
B [MHz]	1161.0474(2)	924.9386(3)	1115.0169(2)	1155.3006(3)	788.2217(9)	959.6477(3)
C [MHz]	997.3061(2)	850.7340(3)	949.2698(2)	1036.7946(4)	765.2924(9)	883.4987(3)
D_J [kHz]	1.555(3)	0.428(3)	2.589(2)	3.486(7)	0.404(4)	1.071(3)
D_{JK} [kHz]	−5.16(2)	9.29(1)	−4.35(2)	−7.94(3)	−7.00(5)	−8.19(4)
d_1 [kHz]	−0.246(2)	−0.042(3)	−0.655(2)	−1.056(7)	−0.044(6)	−0.198(3)
d_2 [kHz]	−0.018(2)	−0.011(2)	−0.044(3)	−0.094(5)	0.007(3)	−0.017(3)
σ [kHz][c]	1.9	2.3	1.5	2.2	5.2	2.1
			D isotopomers[d]			
A [MHz]	4286.580(2)	5168.0(6)	4232.520(2)	4001.503(4)	7005(10)	5833(14)
B [MHz]	1162.8637(4)	926.1348(7)	11175.464(5)	1158.4317(7)	788.3681(8)	960.919(1)
C [MHz]	998.5287(4)	851.5955(7)	949.7319(6)	1038.6867(7)	765.4632(8)	884.208(1)
σ [kHz][c]	3.8	2.9	4.0	3.7	4.4	5.2

[a] D_K was fixed at 0.0 in all fits. [b] Standard errors (in parentheses) are expressed in units of the last digits. [c] Root-mean-square (rms) deviation of the fit. [d] The centrifugal distortion constants of H- and D-isotopomers are similar, and the latter are omitted here. A complete list is given in Table S2 in the Supporting Information.

effect on the moments of inertia upon isotopic substitution. The reduction of the effective bond distance (r_0) due to the ZPE effect outweighs the mass increase of the heavier isotopomer. However, this reversed frequency pattern was not observed for the closely related molecular adducts PO···H_2O and PO···D_2O, in which a similar O···H–O hydrogen bond is present.[25] We therefore concluded that the hydroxy H atom is located fairly close to the center of mass of the molecular adduct and that the zero-point vibrational effect is magnified dramatically. An exact determination of the position of the hydroxy proton relative to the center of mass by a Kraitchman analysis[26] would therefore not lead to a meaningful value and was not pursued further.

The calculated rotational constants are in fairly good agreement with the experimentally determined values, with a maximum deviation of 64 MHz or 7%. Reasonable agreement was also noted for the experimental and calculated electric dipole moment components. The six sets of experimental rotational constants could therefore be assigned unambiguously to the six distinct conformers. We can also infer that the actual geometries of these conformers are close to the predicted ones.

Hydrogen-bond formation from the EtOH hydroxy group to either oxygen lone pair of PO introduces a new stereocenter that can lead to *syn* or *anti* conformations. This additional transient chiral stereogenic center brings the total number of stereocenters in the complex to three. Therefore, two different mechanisms of chiral recognition are present in the PO···EtOH molecular adduct. The first involves the chirality of the two binding partners, for example, (*R*)-PO with two helical forms, that is, the *G+* and *G−* forms of EtOH, and is referred to as diastereomeric discrimination, in line with the definition used in Reference [6]. (*T*)-EtOH, however, does not exhibit diastereomeric discrimination by definition. The energy differences caused by the binding dissimilarity on the *syn* and the *anti* side of PO are referred to as diastereofacial contribution. For example, diastereofacial discrimination is at play in the PO···H_2O adduct and the experimental intensity ratio of *anti* versus *syn* conformers is approximately 1:1.8, indicating a preference for the *syn* conformer.[25] The diastereofacial discrimination exists for all *syn* and *anti* pairs of the PO···EtOH complex.

The strength of the current study lies in the fact that all six possible hydrogen-bonded conformers were captured experimentally and a comprehensive analysis of the chiral discrimination interactions can be accomplished on the basis of the conformational stability. The experimental conformational stability ordering was extracted from the observed intensity ratios of the same rotational transition, taking into account their respective dipole moment strength. Quantitative analyses of the relative energies were reported previously with jet rotational spectroscopic studies, for example, for glycolamide monomer.[27] In the present case, the observed higher abundance of *syn G−* relative to *syn G+* is a clear indication that the former is energetically favored, as both (*G−*)- and (*G+*)-EtOH monomers have the same pre-expansion abundance. It is difficult, however, to obtain precise information on the degree of conformational relaxation in a jet expansion without a systematic investigation that involves changing source temperatures and carrier gases, and theoretical modeling of conformational barrier heights. We therefore restrict our analysis to the clear stability trend observed. The experimental stability ordering of the conformers was established to be *syn G− < anti G− < syn T* ≈ *syn G+ < anti G+ < anti T*. From the experimental ordering, the effect of chiral discrimination, that is, the preference of homo- or heterochiral combination, was determined. Table 3 summarizes the experimentally determined signs of the chirodiastaltic energies and compares them to those predicted by the MP2/6-311++G(d,p) calculations. The contributions of the diastereomeric and diastereofacial effects are analyzed separately. The diastereomeric chirodiastaltic energy is defined as $\Delta E_{chir}(\text{diastereomeric}) = E(\text{het}) - E(\text{hom})$. The heterochiral conformers involving (*R*)-PO and (*G−*)-EtOH are observed to be more stable, in agreement with the positive ΔE_{chir} values calculated using ΔD_e or ΔD_0 values without BSSE corrections. We note that inclusion of the BSSE corrections alters the stability ordering and results in less favorable agreement

Table 3: Comparison of the experimental relative stabilities with the calculated chirodiastaltic energies (ΔE_{chir}), separated into diastereomeric and diastereofacial contributions, at the MP2/6–311++G(d,p) level.

Diastereomers	ΔE_{chir} ΔD_e	ΔD_0	ΔD_0(BSSE)[a]	sign[b]
E(het)−E(hom) = ΔE_{chir}(diastereomeric)				
(*anti G*−)−(*anti G*+)	0.49	0.37	−0.32	+
(*syn G*−)−(*syn G*+)	0.30	0.29	0.20	+
E(*syn*)−E(*anti*) = ΔE_{chir}(diastereofacial)				
(*syn G*−)−(*anti G*−)	0.39	0.24	0.49	+
(*syn T*)−(*anti T*)	0.48	0.24	−0.13	+
(*syn G*+)−(*anti G*+)	0.59	0.32	−0.03	+

[a] Includes BSSE correction. [b] Determined experimentally. See text for details.

with the experimental observation. The discrimination here occurs largely through different degrees of steric hindrance caused by the different spatial orientations of the methyl groups in (*G*+)- and (*G*−)-EtOH. The diastereofacial discrimination energies, defined as ΔE_{chir}(diastereofacial) = E(*syn*)−E(*anti*), were calculated for each conformer pair involving (*G*−)-, (*G*+)-, or (*T*)-EtOH. In this case, a preference of the *syn* side is found experimentally. Again, the more consistent agreement with the experimental observations exist for the calculations without BSSE corrections. Diastereofacial chiral discrimination takes place mainly through the intermolecular interactions of the PO methyl group with the oxygen atom of EtOH through the formation of different secondary C–H···O hydrogen bonds.[28] A similar conclusion was reached for the related PO···H_2O molecular adduct.[25]

In summary, rotational spectra of all six possible hydrogen-bonded PO···EtOH conformers were detected and analyzed for both EtOH and EtOD isotopomers. The chiral discriminating forces at play were examined with complementary high-level ab initio calculations. Overall, a clear stability ordering of the conformers was extracted from the experiment. The theoretical stability ordering showed, however, poor agreement with the observations when the BSSE corrections were included. Unlike in the classic lock-and-key picture, in which steric hindrance is a major player, it is the concerted effect of secondary hydrogen-bond interactions and steric hindrance that seems to govern the discrimination process in this microscopic example, leading to a preference of the *syn* conformation and the heterochiral combination. This present study is one of the first few reports that demonstrate the great potential of high-resolution spectroscopy for exploring the underlying mechanism of molecular recognition in the gas phase.

Experimental Section

The sample mixtures consisted of 0.15% EtOH or EtOD and 0.15% PO in neon at a stagnation pressure of 3.0–6.0 bars. EtOH (99% purity, Fluka), EtOD (99% purity, Fluka), (*R*)-PO (99% purity, Acros), and neon (99.9990%) were used without further purification. The rotational spectrum was recorded in the frequency range of 3.5–15.0 GHz with a Balle–Flygare type[29] pulsed molecular beam Fourier transform microwave spectrometer, which has been described previously.[30] The experimental uncertainty in the rotational transition frequencies is estimated to be about 1 kHz. The full line width at half height is about 10 kHz for well-resolved lines.

Received: September 15, 2006
Published online: November 17, 2006

Keywords: ab initio calculations · chirality · hydrogen bonds · molecular recognition · rotational spectroscopy

[1] E. Fischer, *Ber. Dtsch. Chem. Ges.* **1894**, *27*, 2985–2993.
[2] C. Hunter, *Angew. Chem.* **2004**, *116*, 5424–5439; *Angew. Chem. Int. Ed.* **2004**, *43*, 5310–5324.
[3] H. Gohlke, G. Klebe, *Angew. Chem.* **2002**, *114*, 2764–2798; *Angew. Chem. Int. Ed.* **2002**, *41*, 2644–2676.
[4] Y. Xu, W. Jäger, *J. Chem. Phys.* **1997**, *107*, 4788–4796.
[5] D. P. Craig, D. P. Mellor, *Top. Curr. Chem.* **1976**, *63*, 1–48.
[6] S. Portmann, A. Inauen, H. P. Lüthi, S. Leutwyler, *J. Chem. Phys.* **2000**, *113*, 9577–9585.
[7] A. R. Al-Rabaa, E. Bréhéret, F. Lahmani, A. Zehnacker, *Chem. Phys. Lett.* **1995**, *237*, 480–484.
[8] S. Piccirillo, C. Bosman, D. Toja, A. Giardini-Guidoni, M. Pierini, A. Troiani, M. Speranza, *Angew. Chem.* **1997**, *109*, 1816–1818; *Angew. Chem. Int. Ed. Engl.* **1997**, *36*, 1729–1731.
[9] a) N. Borho, M. Suhm, *Phys. Chem. Chem. Phys.* **2002**, *4*, 2721–2732; b) T. B. Adler, N. Borho, M. Reiher, M. A. Suhm, *Angew. Chem.* **2006**, *118*, 3518–3523; *Angew. Chem. Int. Ed.* **2006**, *45*, 3440–3445.
[10] A. K. King, B. J. Howard, *Chem. Phys. Lett.* **2001**, *348*, 343–349.
[11] J. P. Hearn, R. V. Cobley, B. J. Howard, *J. Chem. Phys.* **2005**, *123*, 134324.
[12] Z. Su, N. Borho, Y. Xu, *J. Am. Chem. Soc.* **2006**, in press.
[13] a) J. C. Pearson, K. V. L. N. Sastry, M. Winnewisser, E. Herbst, F. C. De Lucia, *J. Phys. Chem. Ref. Data* **1995**, *24*, 1–32; b) J. C. Pearson, K. V. L. N. Sastry, E. Herbst, F. C. De Lucia, *J. Mol. Spectrosc.* **1996**, *175*, 246–261.
[14] Gaussian 03 (Revision B.01): M. J. Frisch et al., see Supporting Information.
[15] J. S. Binkley, J. A. Pople, *Int. J. Quantum Chem.* **1975**, *9*, 229–236.
[16] R. Krishman, J. S. Binkley, R. Seeger, J. A. Pople, *J. Chem. Phys.* **1980**, *72*, 650–654.
[17] S. F. Boys, F. Bernardi, *Mol. Phys.* **1970**, *10*, 553–566.
[18] J. D. Swalen, D. R. Herschbach, *J. Chem. Phys.* **1957**, *27*, 100–108.
[19] D. R. Herschbach, J. D. Swalen, *J. Chem. Phys.* **1958**, *29*, 761–776.
[20] M. Imachi, R. L. Kuczkowski, *J. Mol. Struct.* **1982**, *96*, 55–60.
[21] R. K. Kakar, C. R. Quade, *J. Chem. Phys.* **1980**, *72*, 4300–4307.
[22] S. Blanco, A. Maris, S. Melandri, W. Caminati, *Mol. Phys.* **2002**, *100*, 3245–3249.
[23] Z. Su, Y. Xu, *J. Mol. Spectrosc.* **2005**, *232*, 112–114.
[24] Y. Liu, W. Jäger, *Mol. Phys.* **2002** *100*, 611–622.
[25] Z. Su, Q. Wen, Y. Xu, *J. Am. Chem. Soc.* **2006**, *128*, 6755–6760.
[26] J. Kraitchman, *Am. J. Phys.* **1953**, *21*, 17–24.
[27] A. Maris, *Phys. Chem. Chem. Phys.* **2004**, *6*, 2611–2616.
[28] G. R. Desiraju, T. Steiner, *Oxford University Press*, Oxford, **1999**.
[29] T. J. Balle, W. H. Flygare, *Rev. Sci. Instrum.* **1981**, *52*, 33.
[30] Y. Xu, W. Jäger, *J. Chem. Phys.* **1997**, *106*, 7968–7980.

